Available online at www.sciencedirect.com
ScienceDirect
Computers and Structures 86 (2008) 1503–1516
Computers & Structures
www.elsevier.com/locate/compstruc

Race driver model

F. Braghin, F. Cheli, S. Melzi, E. Sabbioni *

Politecnico di Milano, Department of Mechanics, Via La Masa 34, 20158 Milan, Italy

Received 5 March 2007; accepted 30 April 2007
Available online 20 March 2008

Abstract

The best race driver is the one that, with a given vehicle, is able to drive on a given track in the shortest possible time. Thus, the only target is the lap time. A race driver model has to do the same.

The first step towards this target is to decide which trajectory to follow. In fact, the optimal trajectory is the best compromise between the shortest track and the track that allows to achieve the highest speeds (least curvature track). Thus, the problem of trajectory planning is a bounded optimisation problem that has to take into account not only the geometry of the circuit but also the dynamics of the vehicle. A simplified vehicle dynamic model is used for this purpose. Due to the fact that the vehicle will be driven at its limit performances, although simplified, the model has to correctly reproduce the maximum possible acceleration, a function of the vehicle speed, the maximum possible deceleration, again a function of the vehicle speed, and the maximum lateral acceleration, a function of both the vehicle speed and the steering angle. Knowing the trajectory, the vehicle model allows to determine the lap time. Through an optimisation algorithm it is therefore possible to determine the best compromise between shortest track and track with the minimum curvature, i.e. the trajectory (in terms of track and speed profile) that allows to minimize the time lap.

Once the best trajectory has been determined (both in terms of best track and best speed profile), it is necessary to identify the driver's inputs to follow the given trajectory. This task is carried out by considering the driver as a controller that acts on a nonlinear plant (the vehicle) in order to achieve the desired results. Thus, the driver converts the best trajectory into vehicle's inputs. The mutual interaction between plant and controller (the driver's inputs are not only a function of the best trajectory but also of the driver's reactions due to the vehicle's dynamics) is not taken into account in this paper.

Keywords: Race driver; Numerical model; Trajectory planning; Driver's inputs

1. Introduction

A race driver should be able to push a racing car at its highest performance exploiting all the friction forces developed at the tire–road interface according to the constraints imposed by the handling characteristics of the vehicle and by the available traction/braking power.

A mathematical model of a race driver represents an important tool for the development of a race car at a design stage since it actually could provide information about the effective potential of a racing car, drawing guidelines for the trade-off among different solutions. Moreover cost benefits could be achieved since expensive activities such as set-up definition (adjustment of suspensions' parameters, anti-roll bar tuning, settings of aerodynamics devices) could be partially carried out in a virtual environment. Thus, a driver model might also be useful to identify the optimal vehicle set-up to obtain the best lap time on a determined circuit with an assigned racing car.

The first step to design a race driver model is represented by trajectory planning, i.e. the definition of the optimal trajectory that allows to obtain the lowest lap time. This problem has been investigated by several authors [1–4] focusing the attention on car-like robots. Unfortunately in many cases the trajectory planning is considered a purely geometrical problem, regardless of the vehicle's dynamics. Instead, the optimal trajectory is the best compromise between the shortest track and the track that allows to achieve the

* Corresponding author.
E-mail address: edoardo.sabbioni@polimi.it (E. Sabbioni).

0045-7949/$ - see front matter © 2008 Elsevier Ltd. All rights reserved.
doi:10.1016/j.compstruc.2007.04.028

highest speeds (least curvature track). What determines the weight between these two solutions is the vehicle's dynamic behaviour. As an example, a least curvature trajectory allows higher speeds, but if the engine does not provide enough power to reach such speeds, a shorter trajectory should be preferred.

Once the optimal trajectory and speed profile have been determined, it is necessary to convert them into driver's inputs. This is done by considering the driver as a controller that has the possibility to change some vehicle's inputs (gear, clutch, brake, accelerator and steer wheel angle) in order to follow the planned trajectory [5]. It can be clearly seen that these inputs have to take into account the dynamics of the vehicle.

It should be considered that, for a real driver, inputs are not only a function of the planned trajectory but also of the vehicle's dynamics that, as already said, is a function of these inputs. Thus, a third layer has to be added to the trajectory planning phase and the identification of driver's inputs phase, i.e. the optimisation of driver's inputs phase. This third layer allows to further optimise the lap time, by taking into account both the vehicle performances and the driver's reactions, and to achieve a driver's behaviour that is very similar to real one [6].

2. Trajectory planning

The goal of a race driver can be easily described: minimize the lap time. Two strategies can be followed to reach this task: minimize the space and/or maximize the speed. The maximum speed $v_{\max}$ achievable while negotiating a curve of radius ρ is limited by the maximum centripetal force developed by the tires which can be estimated as follows:

$$ma_{y,\max} = m\frac{v_{\max}^2}{\rho} = \mu(mg + F_a);$$
$$\Rightarrow \quad v_{\max} = \sqrt{\mu\rho\left(g + \frac{F_a}{m}\right)} \tag{1}$$

In (1) m represents the vehicle's mass, μ the tire–road friction coefficient, F_a the aerodynamic downforce. Relation (1) shows that the two strategies of space minimization and speed maximization are conflicting: the shortest path approach leads to a trajectory characterized by low curvature radii while the highest speed approach pushes towards high curvature radii (i.e. the minimization of curvature).

Fig. 1 should clarify the situation: the minimum space trajectory (a) presents the lowest curvature radius; trajectory (b) is characterized by the largest curvature radius (minimum curvature) and allows to negotiate the curve at the maximum speed, but presents a sensible increase of space. The solution that leads to the lowest lap time is a compromise between trajectory (a) and (b) and is strictly dependent on the vehicle's dynamics. The tire–road adhesion condition might make it impossible to follow trajectory (a) except at very low speeds. At the same time, the engine might not be able to produce the required driving torque and thus the speed allowed by trajectory (b).

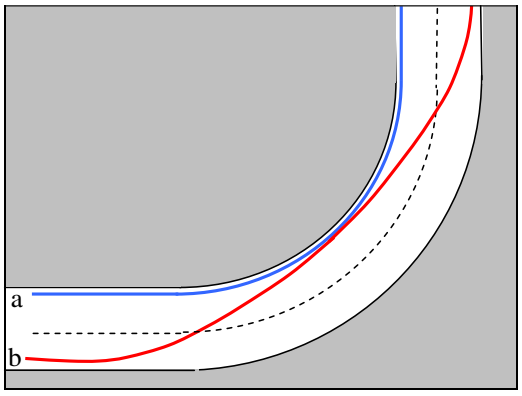

Fig. 1. Comparison between shortest space (a) and lowest curvature (b) trajectories.

According to the approach followed in this work, at first the pure geometrical problem is analyzed. Algorithms are developed to identify the shortest path and the trajectory with the lowest curvature given the track centerline trajectory and the road width. Then, a simplified vehicle model is used to identify the most appropriate weights for the two solutions thus allowing to determine the optimal path and the corresponding speed profile.

3. Geometrical problem

Both the algorithms developed to identify the shortest path and the trajectory with the lowest curvature solve a constrained minimization problem since the identified solution has always to be inside the track. The algorithms are based on a discretization of the track into several segments, as shown in Fig. 2.

At the end of each segment the position of a given point on the track is identified using the following equation:

$$\begin{aligned}\vec{\mathbf{P}}_i &= x_i\vec{\mathbf{i}} + y_i\vec{\mathbf{j}} \\ &= [x_{r,i} + \alpha_i(x_{l,i} - x_{r,i})]\vec{\mathbf{i}} + [y_{r,i} + \alpha_i(y_{l,i} - y_{r,i})]\vec{\mathbf{j}} \\ &= [x_{r,i} + \alpha_i\Delta x_i]\vec{\mathbf{i}} + [y_{r,i} + \alpha_i\Delta y_i]\vec{\mathbf{j}}\end{aligned} \tag{2}$$

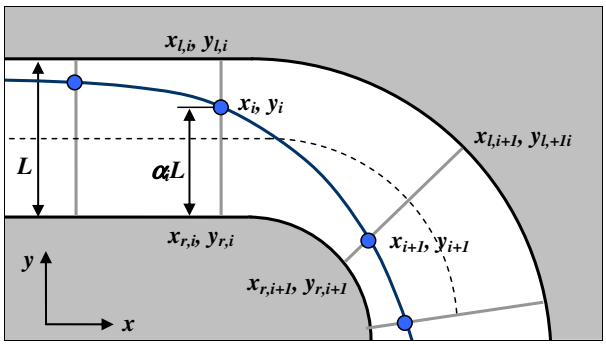

Fig. 2. Trajectory discretization.

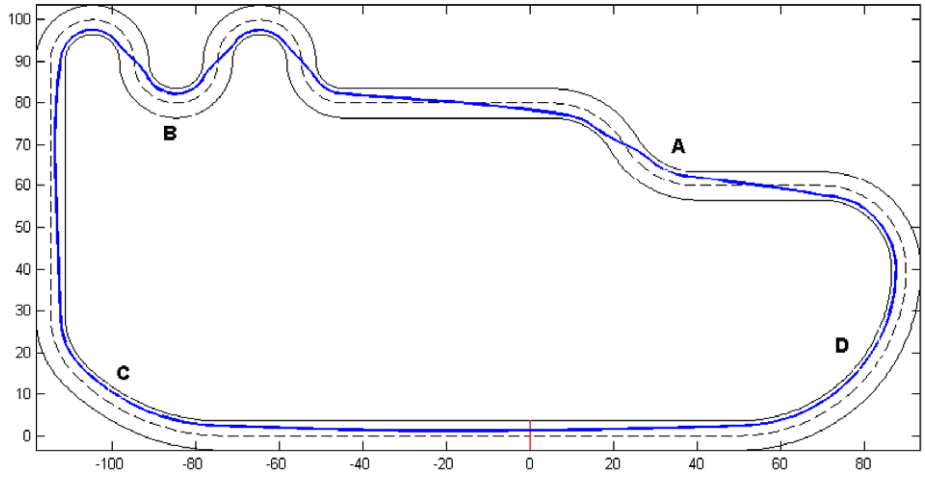

Fig. 3. Minimization result: shortest space trajectory on a test track.

α_i being a parameter that identifies the position of point $\vec{\mathbf{P}}_i$ along the track width. The resulting trajectory will be obtained by linking, through linear (segments) or nonlinear (splines) relations, all the $\vec{\mathbf{P}}_i$ points identified. Thus, the identification of the desired path (shortest or with lowest curvature) can be reduced to the identification of all α_i parameters (independent variables) that can be collected into a vector $\bar{\boldsymbol{\alpha}}$:

$$\bar{\boldsymbol{\alpha}} = \{\alpha_1 \alpha_2 \dots \alpha_n\}^{\mathrm{T}} \tag{3}$$

The range of variation of each element of $\bar{\boldsymbol{\alpha}}$ is clearly [0:1].

3.1. Shortest path trajectory

The easiest way to determine the total path length is to approximate the trajectory with line segments. However, this approach leads to discontinuities in the slope of the trajectory that is important for the calculation of the curvature. By increasing the number of segments in which the track is discretised the problem gets less importance but cannot be eliminated.

The length of the ith segment of the track can be expressed as

$$\vec{\mathbf{P}}_{\mathbf{i}+1} - \vec{\mathbf{P}}_i = \Delta P_{x,i}\vec{\mathbf{i}} + \Delta P_{y,i}\vec{\mathbf{j}} \tag{4}$$

where $\Delta P_{x,i}$ and $\Delta P_{y,i}$ represent the projections of the length of the ith segment along the x and y axes respectively. Eq. (5) expresses these quantities as a function of the independent variables α_i and α_{i+1}:

$$\begin{cases} \Delta P_{x,i} = x_{r,i+1} - x_{r,i} + \alpha_{i+1}\Delta x_{i+1} - \alpha_i \Delta x_i \\ \qquad\quad = [\Delta x_{i+1} - \Delta x_i]\begin{Bmatrix} \alpha_{i+1} \\ \alpha_i \end{Bmatrix} + \Delta x_{i,0} \\ \Delta P_{y,i} = y_{r,i+1} - y_{r,i} + \alpha_{i+1}\Delta y_{i+1} - \alpha_i \Delta y_i \\ \qquad\quad = [\Delta y_{i+1} - \Delta y_i]\begin{Bmatrix} \alpha_{i+1} \\ \alpha_i \end{Bmatrix} + \Delta y_{i,0} \end{cases} \tag{5}$$

being $\bar{\boldsymbol{\alpha}}_i$ the vector $\{\alpha_{i+1} \quad \alpha_i\}^{\mathrm{T}}$. The squared total length of the trajectory is therefore equal to:

$$\begin{aligned} S^2 &= \sum_{i=1}^{n} \Delta P_{x,i}^{\mathrm{T}} \Delta P_{x,i} + \Delta P_{y,i}^{\mathrm{T}} \Delta P_{y,i} \\ &= \sum_{i=1}^{n} \bar{\boldsymbol{\alpha}}_i^{\mathrm{T}} [\mathbf{H}_{S,i}] \bar{\boldsymbol{\alpha}}_i + \{\mathbf{B}_{S,i}\}\bar{\boldsymbol{\alpha}}_i + \mathrm{cost} \end{aligned} \tag{6}$$

the use of appropriate extraction matrices allows to express the squared length of the trajectory as function of the independent variable vector $\bar{\boldsymbol{\alpha}}$:

$$\begin{aligned} S^2 &= \sum_{i=1}^{n} \bar{\boldsymbol{\alpha}}^{\mathrm{T}} [\mathbf{E}_i]^{\mathrm{T}} [\mathbf{H}_{S,i}][\mathbf{E}_i]\bar{\boldsymbol{\alpha}} + \{\mathbf{B}_{S,i}\}[\mathbf{E}_i]\bar{\boldsymbol{\alpha}} + \mathrm{cost} \\ &= \bar{\boldsymbol{\alpha}}^{\mathrm{T}} [\mathbf{H}_S]\bar{\boldsymbol{\alpha}} + \{\mathbf{B}_S\}\bar{\boldsymbol{\alpha}} + \mathrm{cost} \end{aligned} \tag{7}$$

Eq. (7) formulates the search for shortest space problem in a quadratic form. A minimization algorithm can therefore be applied to determine the optimal solution. Fig. 3 shows the results of the described procedure for a test track characterized by a chicane (Section A), a series of short radius curves (Section B), a 90° curve (Section C) and one curve with variable curvature radius (Section D). The solid blue line in Fig. 3[1] represents the shortest path which can be roughly interpreted as a series of arcs of circumference linked by straight lines (Sections B, C, D). It should be noticed that, following the shortest path, the race car has to negotiate curves characterized by very small radii. Thus, to be able to stay on the track, the vehicle's speed has to be drastically reduced when approaching such curves. This leads to high lap times.

3.2. Minimum curvature trajectory

The search for the path characterized by the minimum curvature was at first carried out with an approach similar to the one used to determine the shortest space trajectory. However, preliminary simulations showed that the

[1] For interpretation of color in Figs. 1–13, 15, 16 and 18–23, the reader is referred to the web version of this article.

approximation of the trajectory with a series of segments leads to remarkable errors in the solution of the path with the minimum curvature due to the discontinuities in the slope between adjacent segment. For this reason adjacent points have been connected through closed natural cubic splines [4] to determine the trajectory inside a single segment. This formulation avoids curvature discontinuities in the trajectory

$$\begin{cases} x_i(t) = a_{i,x} + b_{i,x}t + c_{i,x}t^2 + d_{i,x}t^3 \\ y_i(t) = a_{i,y} + b_{i,y}t + c_{i,y}t^2 + d_{i,y}t^3 \\ t(s) = \frac{s-s_{i0}}{ds_i} \end{cases} \tag{8}$$

According to Eq. (8) the trajectory inside one track segment is represented by a third order polynomial function of t; where t represents the curvilinear abscissa normalized to the length of the ith track segment. The track curvature $\hat{\Gamma}$ is determined according to the following expression:

$$\begin{aligned} \hat{\Gamma}^2 &= \left(\frac{\mathrm{d}^2x(s)}{\mathrm{d}s^2}\right)^2 + \left(\frac{\mathrm{d}^2y(s)}{\mathrm{d}s^2}\right)^2 \\ &= \left(\frac{\mathrm{d}^2x(t)}{\mathrm{d}t^2}\left(\frac{\mathrm{d}t(s)}{\mathrm{d}s}\right)^2\right)^2 + \left(\frac{\mathrm{d}^2y(t)}{\mathrm{d}t^2}\left(\frac{\mathrm{d}t(s)}{\mathrm{d}s}\right)^2\right)^2 \\ &= \left(\frac{\mathrm{d}t(s)}{\mathrm{d}s}\right)^4\left[\left(\frac{\mathrm{d}^2x(t)}{\mathrm{d}t^2}\right)^2 + \left(\frac{\mathrm{d}^2y(t)}{\mathrm{d}t^2}\right)^2\right] \end{aligned} \tag{9}$$

If all the segments of the track centerline have the same length $\mathrm{d}s^*$, Eq. (9) simplifies as follows:

$$\left(\frac{\mathrm{d}t(s)}{\mathrm{d}s}\right) = \frac{1}{\mathrm{d}s^*} \quad \Rightarrow \quad \hat{\Gamma}^2 = \left(\frac{1}{\mathrm{d}s^*}\right)^4\left[\left(\frac{\mathrm{d}^2x(t)}{\mathrm{d}t^2}\right)^2 + \left(\frac{\mathrm{d}^2y(t)}{\mathrm{d}t^2}\right)^2\right] \tag{10}$$

The track curvature can thus be minimized considering the quantity Γ^2.

$$\Gamma^2 = \sum_{i=1}^{n}\left[\left(\frac{\mathrm{d}^2x(t)}{\mathrm{d}t^2}\right)^2 + \left(\frac{\mathrm{d}^2y(t)}{\mathrm{d}t^2}\right)^2\right] \tag{11}$$

The second derivative for a closed natural cubic spline, considering variable x computed at $t = 0$, can be expressed as

$$\left.\frac{\mathrm{d}^2\bar{\mathbf{x}}(t)}{\mathrm{d}t^2}\right|_{t=0} = [\mathbf{D}]\bar{\mathbf{x}} \tag{12}$$

where $[\mathbf{D}]$ is a constant matrix while $\bar{\mathbf{x}}$ represents the vector of the components of each point of the trajectory. Considering Eq. (2), vector $\bar{\mathbf{x}}$ linearly depends on the independent variable vector $\bar{\boldsymbol{\alpha}}$:

$$\bar{\mathbf{x}} = \bar{\mathbf{x}}_\mathrm{r} + [\mathbf{dx}]\bar{\boldsymbol{\alpha}} \tag{13}$$

Thus, Eq. (12) can rewritten as

$$\begin{aligned} \left(\left.\frac{\mathrm{d}^2\bar{\mathbf{x}}(t)}{\mathrm{d}t^2}\right|_{t=0}\right)^2 &= \bar{\boldsymbol{\alpha}}^\mathrm{T}([\mathbf{dx}]^\mathrm{T}[\mathbf{D}]^\mathrm{T}[\mathbf{D}][\mathbf{dx}])\bar{\boldsymbol{\alpha}} \\ &\quad + 2\left(\bar{\mathbf{x}}_\mathrm{r}^\mathrm{T}[\mathbf{D}]^\mathrm{T}[\mathbf{D}][\mathbf{dx}]\right)\bar{\boldsymbol{\alpha}} + \bar{\mathbf{x}}_\mathrm{r}^\mathrm{T}[\mathbf{D}]^\mathrm{T}[\mathbf{D}]\bar{\mathbf{x}}_\mathrm{r} \end{aligned} \tag{14}$$

A similar expression can be obtained for the y coordinate so that, considering Eq. (11), Γ^2 can be expressed as a quadratic form of the independent variable vector $\bar{\boldsymbol{\alpha}}$:

$$\Gamma^2 = \bar{\boldsymbol{\alpha}}^\mathrm{T}[\mathbf{H}_\Gamma]\bar{\boldsymbol{\alpha}} + \{\mathbf{B}_\Gamma\}\bar{\boldsymbol{\alpha}} + \mathrm{cost} \tag{15}$$

Fig. 4 shows the result of the minimization procedure applied to the previously described test track. Comparing Figs. 3 and 4 it can be seen that the path with the minimum curvature implies a longer track. This is particularly evident for Sections A, C and D. Despite the disadvantage of a longer path, experience suggests that this solution is usually very close to the optimal one. As described before, the main reason for this is related to the vehicle's dynamics: with a low curvature trajectory the braking action before a turn is less intense since curves can be negotiated at higher

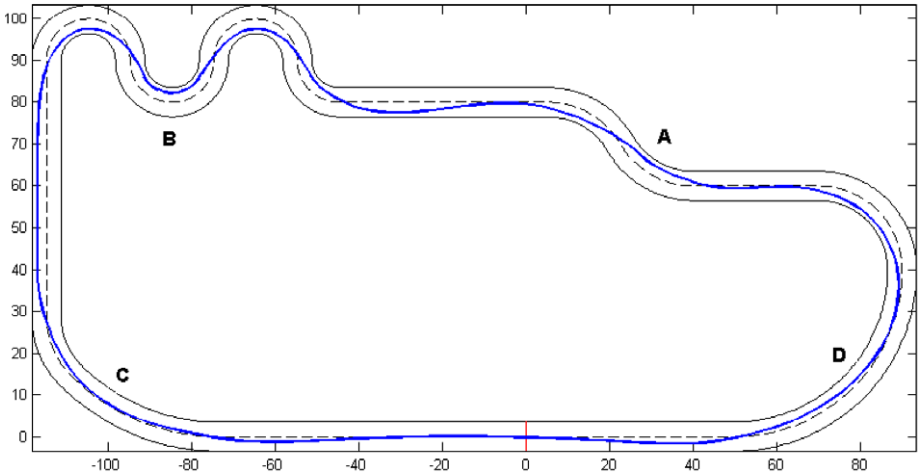

Fig. 4. Minimization result: minimum curvature trajectory on a test track.

speed. Moreover, the throttle valve opening can be anticipated thus leading to smaller speed variations while cornering and to lower lap times.

4. Optimal trajectory: dynamic problem

As already said, the optimal solution is deeply influenced by the dynamic characteristics of the vehicle: the tires' performances, the braking/driving torque available, the presence of aerodynamic devices might induce the race driver to chose a trajectory which can be closer to one of the two solutions. The definition of the optimal trajectory can thus by considered a dynamic problem and another stage of optimisation has to be carried out considering the characteristics of the race car. Assuming that the optimal trajectory is a linear combination between shortest space and minimum curvature, the problem can be analytically formulated by introducing the functional F:

$$F^2 = (1-\varepsilon)\cdot \Gamma^2 + \varepsilon \cdot S^2 \tag{16}$$

that can be rewritten as

$$\begin{aligned} &F^2 = \bar{\boldsymbol{\alpha}}^{\mathrm{T}}[\mathbf{H}]\bar{\boldsymbol{\alpha}} + \{\mathbf{B}\}\bar{\boldsymbol{\alpha}};\\ &[\mathbf{H}] = (1-\varepsilon)[\mathbf{H}_\Gamma] + \varepsilon[\mathbf{H}_s];\\ &[\mathbf{B}] = (1-\varepsilon)\{\mathbf{B}_\Gamma\} + \varepsilon\{\mathbf{B}_s\} \end{aligned} \tag{17}$$

Parameter ε is the weight between the two solutions. The optimal value for ε has to be identified through a minimization procedure with the aim of achieving the lowest lap time. The strategy adopted in this work consists in characterizing the vehicle's performances in terms of maximum lateral/longitudinal accelerations, a function of the vehicle's speed, and making the vehicle follow a trajectory at the highest possible speed. It is therefore possible to associate the best lap time achievable by the examined race car to each value of ε (i.e. to each trajectory). Through a minimization approach, the best lap time is determined together with the best trajectory.

4.1. Dynamic characterization of the vehicle

As a first step a simplified dynamic model of the vehicle has to be introduced. The vehicle is schematized as a material point whose dynamics is characterized by a series of physical limits proper of the considered vehicle. Starting from a detailed numerical model of the racing car, some simple manoeuvres are carried out to characterize the vehicle performances in terms of:

- Maximum lateral acceleration
- Maximum longitudinal acceleration
- Maximum longitudinal deceleration
- Mutual effect of longitudinal/lateral accelerations

Test results are summarized through few curves (e.g. maximum lateral/longitudinal acceleration as function of vehicle speed) which actually constitute the boundary conditions for the minimization algorithm.

The maximum theoretical lateral acceleration achievable while cornering can be estimated through Eq. (1). However, some factors, such as the lateral load transfer while cornering, could sensibly reduce the maximum lateral acceleration. Moreover, due to understeering or oversteering behaviour or to negative camber angles the four tires might be unable to exploit the maximum friction force simultaneously. Therefore, either experimental tests or data coming from a more complex vehicle model, as the one used in this work (a fully nonlinear MB vehicle model), would be preferable.

In order to determine the effective maximum lateral acceleration a series of open-loop steering pad manoeuvres were carried out using a 14 dofs vehicle model [7,8]: keeping the speed of the vehicle constant, the steer angle was slowly increased and the lateral acceleration recorded. The procedure was repeated for a wide range of longitudinal speed. Results are shown in Fig. 5 where the lateral acceleration is plotted as function of both vehicle's speed and steer angle.

As shown in Fig. 6 the maximum lateral acceleration increases with speed due to the aerodynamic downforce effect developed by the considered race car. Simulation results were approximated with a second order polynomial in order to define a smooth boundary condition for the minimization procedure.

As far as the longitudinal dynamics is concerned, the first task is to identify the maximum acceleration developed by the vehicle. This quantity is a function of the engine torque, of the gear ration and of the motion resistances, in particular the drag aerodynamic force. Longitudinal acceleration performance was characterized through a kick down test on straight track with an initial speed equal to zero. The gear shift actuation was optimised in order to get the lowest time required to get from 0 km/h to 200 km/h. Fig. 7 shows the maximum longitudinal acceleration vs. the vehicle speed: the effect of gear shifts is clearly visible. This curve constitutes another boundary condition for the minimization algorithm.

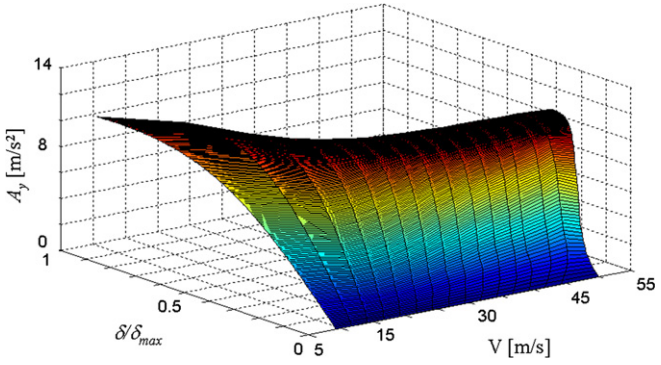

Fig. 5. Lateral acceleration of the racing car as function of speed and steer angle.

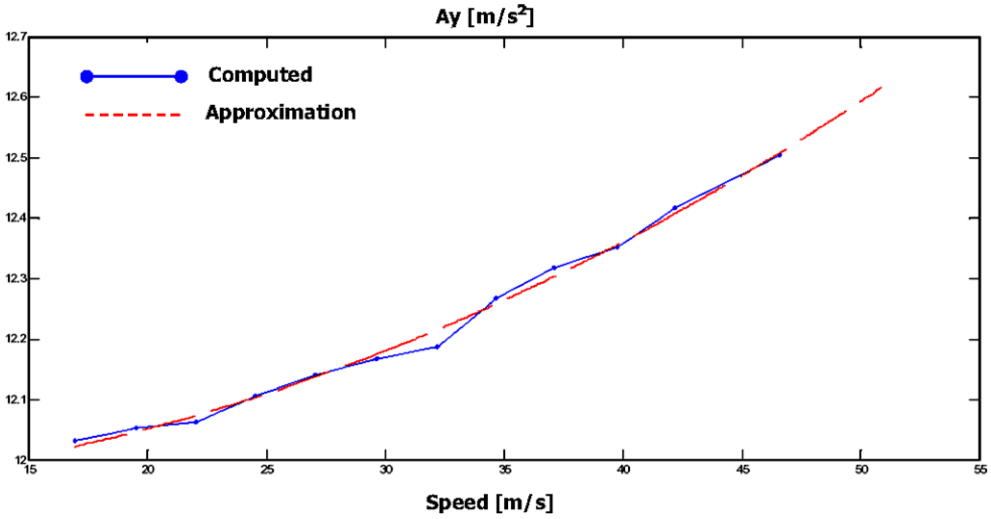

Fig. 6. Maximum lateral acceleration as function of vehicle's speed.

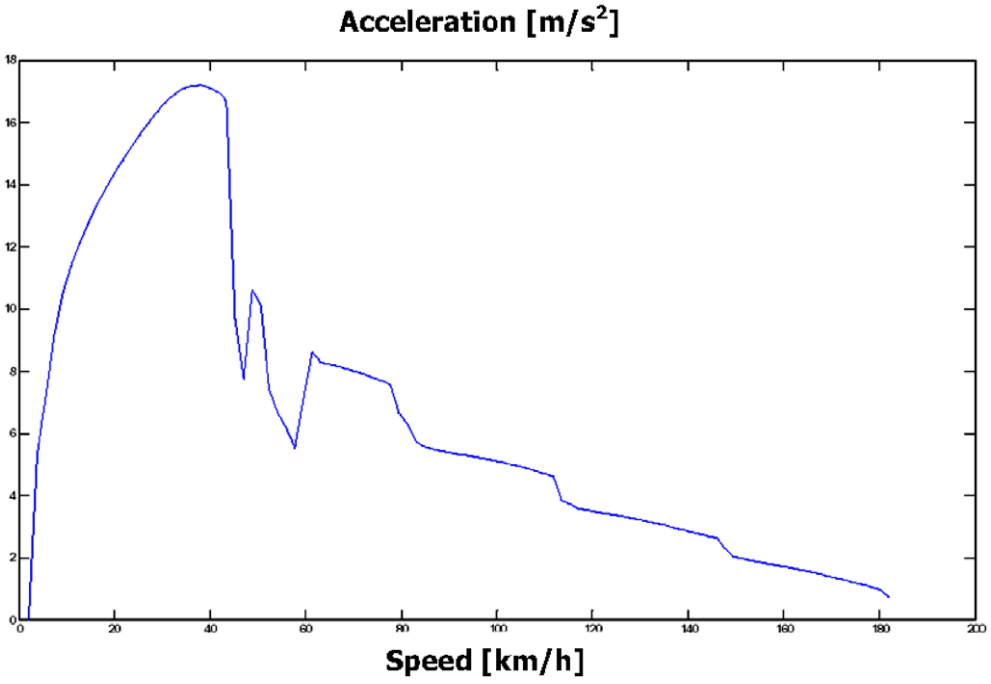

Fig. 7. Maximum racing car longitudinal acceleration as a function of the longitudinal speed.

The characterization of the braking performance was carried out with a similar approach, i.e. considering the application of the maximum braking torque on all tires. Fig. 8 shows the maximum deceleration provided by the braking system. Neither tire-lock nor fading effect were considered.

The last important effect that has to be included among the boundary conditions of the minimization algorithm is the combined slip effect: the global frictional force developed at the tire–road interface cannot grow above a given limit that is a function of the friction coefficient. Eq. (18) is commonly used as a simple saturation model:

$$\left(\frac{\mu_x}{\mu_{x,\max}}\right)^2 + \left(\frac{\mu_y}{\mu_{y,\max}}\right)^2 = 1 \tag{18}$$

In (18) $\mu_{x,\max}$ and $\mu_{y,\max}$ represent the maximum ratios between longitudinal/lateral forces and the normal force respectively; μ_x and μ_y, instead, are the actual ratios between the longitudinal/lateral forces and the normal force. Assuming a linear relation between acceleration and friction coefficient, Eq. (18) can also be rewritten as

$$\left(\frac{a_x}{a_{x,\max}}\right)^2 + \left(\frac{a_y}{a_{y,\max}}\right)^2 = 1 \tag{19}$$

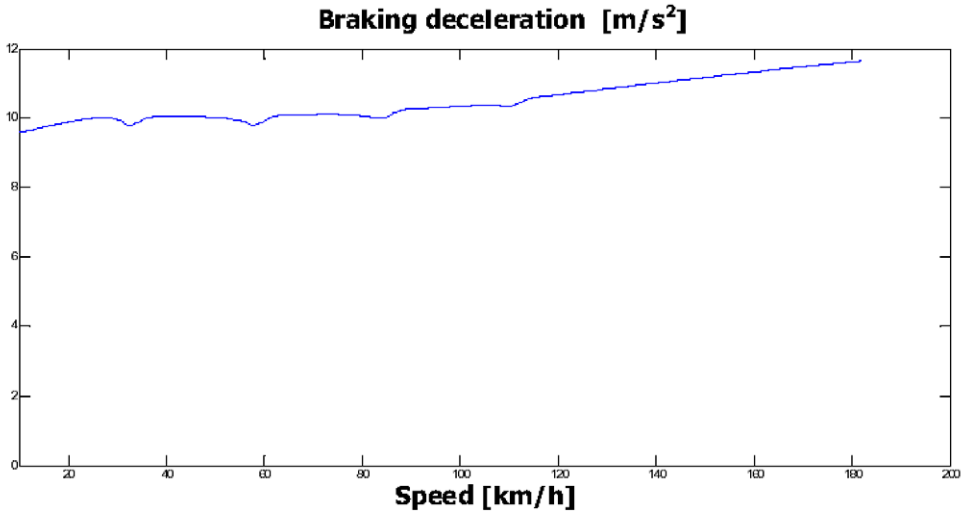

Fig. 8. Maximum racing car longitudinal deceleration as a function of the longitudinal speed.

Eq. (19) represents the last boundary condition of the minimization algorithm.

4.2. Speed profile definition

For a given path (i.e. the parameter ε is assigned), once the vehicle's physical limits have been determined (dynamic characterization of the vehicle), the speed profile, a function of the curvilinear abscissa $v(s)$, has to be identified in order to determine the lap time. The starting speed profile is given by the maximum lateral acceleration: the maximum vehicle speed at the ith point along the track (see Fig. 2) has to satisfy the following equation:

$$\frac{v_{i,\max}^2}{\rho_i} = a_{yi,\max}(v) \tag{20}$$

where ρ_i is the local curvature radius and the function $a_{yi,\max}(v)$ is the previously defined maximum lateral acceleration for the given vehicle. However, the obtained speed profile does not consider the space needed to accelerate/decelerate the vehicle and neglects the simultaneous application of longitudinal and lateral forces. These limits can be introduced through the following equations:

$$\begin{cases} a_{x,i} = \min\left[a_x(v_i), a_{x,\max}\sqrt{1-\left(\frac{a_{y,i}}{a_{y,\max}}\right)}\right] & \text{acceleration} \\ a_{x,i} = \max\left[a_x(v_i), a_{x,\max}\sqrt{1-\left(\frac{a_{y,i}}{a_{y,\max}}\right)}\right] & \text{braking} \end{cases} \tag{21}$$

In (21) $a_x(v_i)$ represents the maximum longitudinal acceleration developed by the vehicle as a function of the vehicle speed; $a_{x,i}$ and $a_{y,i}$ are the longitudinal and the lateral acceleration at the ith point of the trajectory respectively, while $a_{x,\max}$ and $a_{y,\max}$ are the maximum longitudinal and lateral acceleration imposed by the adhesion limit.

Fig. 9 shows an example of the speed profile for a left hand curve. Line A is referred to the speed profile generated only according to Eq. (20). In this case the vehicle approaches the curve at maximum speed (around

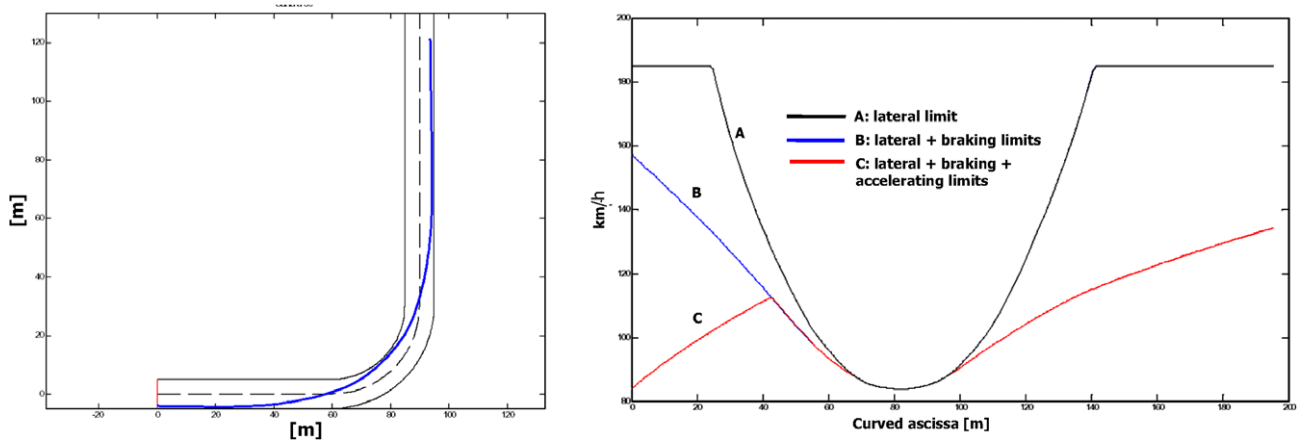

Fig. 9. Steps of speed profile definition for a left hand turn.

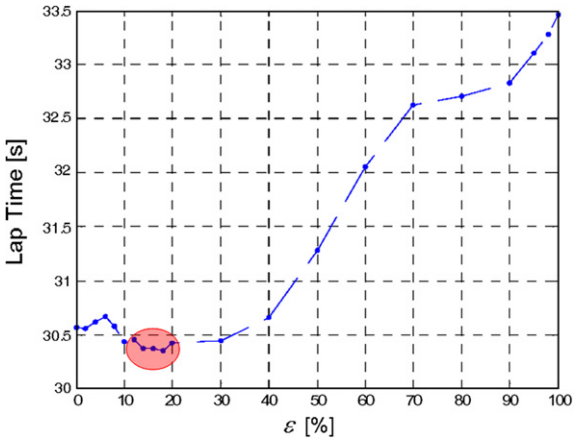

Fig. 10. Lap time on the test track as function of the weight ε.

180 km/h), then brakes and accelerates simply according to the local curvature radius. Line B considers the efficiency of the braking system: since it is physically impossible to enter the curve at 180 km/h, the initial speed has to be reduced to about 160 km/h. At last, line C introduces the acceleration performance of the car considering an initial speed of 83 km/h (due to a previous curve).

4.3. Optimal trajectory

Determining a speed profile allows to estimate the lap time achievable by a specific vehicle on a given track. The comparison among all the lap times obtained for different values of parameter ε allows to identify the minimum lap time and thus the optimal trajectory.

Fig. 10 shows the best lap time obtained by the considered race car on the test track (see Figs. 3 and 4) as a function of the parameter ε. As can be noticed, the lowest lap time (30.35 s) is obtained when the weight ε is about 0.15 (this is only an analytical solution, however values of ε comprised within the range [0–0.2] give similar results). Thus the minimum curvature trajectory is the most weighted. The shortest path trajectory, in fact, leads to a lap time of 33.5 s, about 3 s slower than the optimal solution. Then the result of the optimisation procedure seems to confirm the common experience that the best lap corresponds to the trajectory with the minimum curvature.

5. Driver's inputs identification

In order to follow the desired trajectory and speed profile, the driver can act on the following inputs:

- gear;
- clutch;
- accelerator;
- brake;
- steer wheel angle.

5.1. Gear shift and clutch actuation

The gear is used to have a driving torque available at any time instant. Therefore, the gear should be shifted whenever the driving torque is different form the maximum available. However, shifting the gear requires time during which no driving torque is applied to the wheels. It was therefore decided to implement an automatic gear shift that allows to achieve the best compromise between maximum driving torque available at the wheels and minimum latency time, i.e. to achieve the best lap time.

As shown by experience, lap time is much more affected by an erroneous actuation of the brakes and/or of the accelerator than by an erroneous choice of the instant at which the gear is shifted. Thus, the control logic of the automatic gear shift is very simple: during acceleration the gear is incremented when the engine speed reaches the value that corresponds to the maximum engine torque for that gear while during deceleration the gear is decremented when the engine speed reaches the value

$$\mathrm{rpm}_{i\_\max} \cdot \frac{\tau_{i-1}}{\tau_i} \tag{22}$$

where $\mathrm{rpm}_{i\_\max}$ is the engine speed that corresponds to the maximum engine torque for ith gear, τ_i is the transmission ratio of the actual gear and τ_{i-1} is the transmission ratio of the lower gear. It should be observed that multiple gear shifts are not allowed by the implemented algorithm.

In order to obtain the best lap time, the clutch actuation time should be the shortest possible. Thus, no optimisation is necessary. However, the clutch actuation time is a function of the driver's promptness and of the clutch type. It was therefore decided to model the clutch's dynamics as a first order system and to add a constant latency time (assumed equal to 0.5 s) to reproduce the driver's promptness.

5.2. Accelerator and brakes

Fig. 11 gives an overview of the control logic used to determine the accelerator (α) and the brake (γ) inputs as a function of the vehicle's speed profile. A feed-forward contribution (α_{FF},γ_{FF}) based on a simplified vehicle model and a feed-back contribution (α_{FB},γ_{FB}) are considered.

5.2.1. Feed-forward contribution

The feed-forward contribution allows to improve the promptness of the driver. The accelerator and brake feed-forward inputs are determined using a very simple 1 dof vehicle model whose equation of motion is

$$\begin{aligned} &M \cdot a_{x\_\mathrm{ref}} + 4J_{\mathrm{r}} \frac{a_{x\_\mathrm{ref}}}{R^2} + 4J_{\mathrm{m}} \frac{a_{x\_\mathrm{ref}}}{R^2 \cdot \tau^2} + \frac{1}{2}\rho C_x A \cdot V_{\mathrm{ref}}^2 \\ &\quad = \alpha_{\mathrm{FF}} \cdot \frac{C_{m\_\max}(\omega_{\mathrm{m}}) + C_{m\_\min}(\omega_{\mathrm{m}})}{R \cdot \tau} - \frac{C_{m\_\min}(\omega_{\mathrm{m}})}{R \cdot \tau} \end{aligned} \tag{23}$$

where M is the vehicle's mass, J_{r} is wheels moment of inertia, R is the wheels radius, J_{m} is the engine moment of iner-

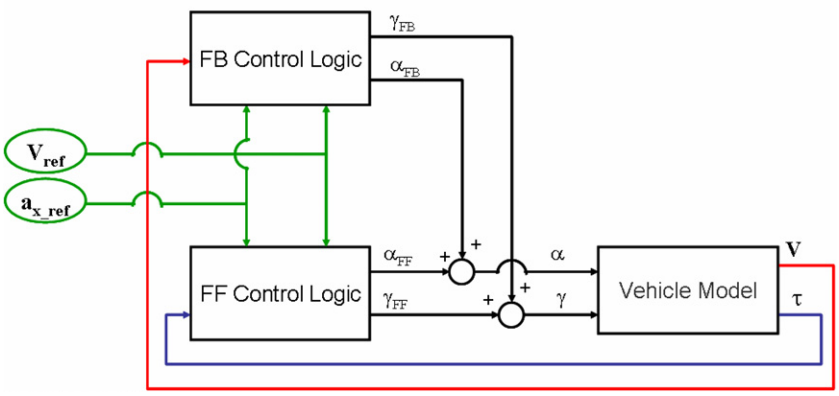

Fig. 11. Scheme of the control logic for brake and accelerator.

tia, ρ is the air density, A is the vehicle frontal area, τ is transmission ratio, C_m is the engine torque (a function of the engine angular speed), ω_m is the engine angular speed ($\omega_m = V_{ref}/(R\tau)$), V_{ref} and a_{x_ref} are the reference speed and the longitudinal acceleration determined during the trajectory planning phase and α_{FF} is the accelerator input, expressed as a fraction of the full throttle admission.

During braking a similar equation of motion can be written:

$$M \cdot a_{x\_ref} + 4J_r \frac{a_{x\_ref}}{R^2} + 4J_m \frac{a_{x\_ref}}{R^2 \cdot \tau^2} = \gamma_{FF} \cdot \left(\frac{C_{front} + C_{rear}}{R}\right) + \frac{1}{2}\rho C_x A \cdot V_{ref}^2 - \frac{C_{m\_min}(\omega_m)}{R \cdot \tau} \tag{24}$$

where C_{front} and C_{rear} are two constants that allow to transform the brake input γ_{FF} into braking torques at the front and rear axles.

Through Eqs. (23) and (24) the feed-forward accelerator and the brake inputs are estimated. However, the vehicle model upon which the controller is based (1 dof vehicle model) is too simplified to guarantee that the reference speed profile is exactly followed. Thus a feed-back contribution has to be added.

5.2.2. Feed-back contribution

In order to reduce the error between the reference speed profile and the actual speed profile of the vehicle, two PI (proportional–integrative) controllers have been implemented, one for the accelerator (α_{FB}) input and one for the brake (γ_{FB}) input:

$$\begin{aligned} \alpha_{FB} &= k_{\alpha p} \cdot (V_{ref} - V) + k_{\alpha i} \cdot \int (V_{ref} - V)\mathrm{d}t \\ \gamma_{FB} &= k_{\gamma p} \cdot (V_{ref} - V) + k_{\gamma i} \cdot \int (V_{ref} - V)\mathrm{d}t \end{aligned} \tag{25}$$

In Eq. (25) $k_{\alpha p}$, $k_{\alpha i}$, $k_{\gamma p}$ and $k_{\gamma i}$ are the controller gains and V is the actual speed of the vehicle. The optimisation of the controller gains has been carried out iteratively considering a fully nonlinear 14 dofs vehicle model [7,8]. Being the driver model a race driver model, the optimal solution is the one that allows to exactly reproduce the speed reference determined during the trajectory planning phase. A set of gains that allows to almost achieve the best lap with smooth accelerator and brake actions is preferable with respect to a set of gains that allows to achieve the best lap but with very nervous accelerator and brake actions.

In order to further improve the reference speed following target and to obtain smooth driver's inputs, a "visual distance" has been introduced:

$$l_{acc/brake} = V_{ref} T_v - \frac{1}{2} a_{x\_ref} T_v^2 \tag{26}$$

where T_v is the visual distance gain that has been optimised through iterations. In fact, this parameter has a physical meaning since it allows to numerically reproduce the fact that the driver sets up the manoeuvre some seconds (meters) in advance. Once this gain has been identified, knowing the actual reference vehicle speed and longitudinal acceleration, the "visual distance" can be calculated. Then, for both the feed-forward and feed-back contributions the reference speed (longitudinal acceleration) used is not the actual one but the one that the vehicle will have $l_{acc/brake}$ meters in front.

The test circuit used to determine the best set of controller gains is the one shown in Fig. 4. It is made of a series of large and small radius curves and straight tracks that allow to easily evaluate the race driver behaviour both in terms of trajectory planning and driver's inputs identification. Fig. 12 shows the normalized (with respect to their maximum value) accelerator and brake inputs on this test track that correspond to the best set of controller gains. Also the reference speed profile and the actual one are shown. A mean square error of 0.8% is obtained. It should be noticed that, by further increasing $k_{\alpha p}$ and $k_{\gamma p}$ gains, the mean square error can be further reduced but the driver inputs become more and more nervous.

5.3. Steer wheel angle

In order to identify the input for steer wheel angle that allows to follow the desired trajectory, two error functions have been defined:

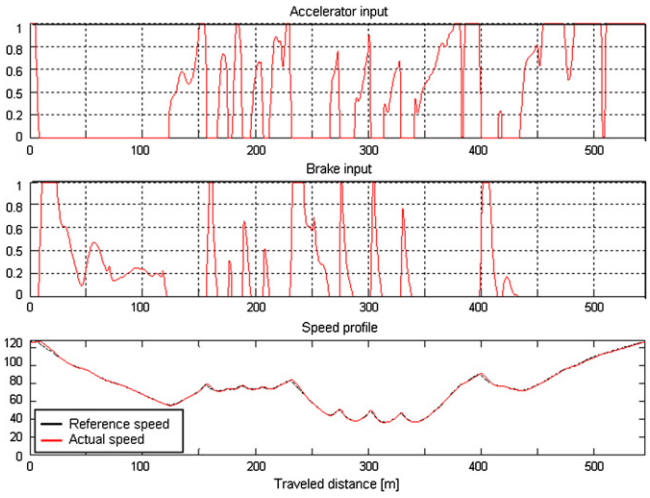

Fig. 12. Time histories of accelerator, brake and vehicle speed (compared to the reference speed) for the test circuit shown in Fig. 4.

$$\begin{aligned} e_1 &= \Delta\sigma = \sigma_{\text{ref}}(s + l_{\text{steer}}) - \sigma(s) \\ e_2 &= d = [P_{G\_x}(s) - P_{\text{ref}\_x}(s)] \cdot \cos(\sigma_{\text{ref}}(s)) \\ &\quad + [P_{G\_y}(s) - P_{\text{ref}\_y}(s)] \cdot \sin(\sigma_{\text{ref}}(s)) \end{aligned} \tag{27}$$

where σ_{ref} is the tangent direction to the ideal path (determined during the trajectory planning phase), a function of the curvilinear abscissa s along the path and of the "visual distance" l_{steer} that will be explained further on, and σ is the inclination of the vehicle's longitudinal axis with respect to a given absolute reference system, while P_{G_x}, P_{G_y}, P_{ref_x} and P_{ref_y} are the coordinates of the vehicle's cog and of the corresponding position on the reference path respectively. Fig. 13 graphically shows the quantities that appear in the two error functions defined in Eq. (27).

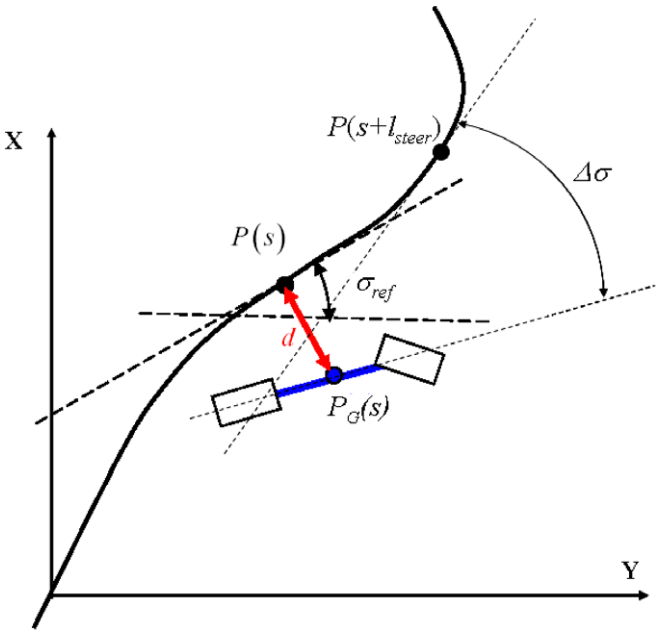

Fig. 13. Steer wheel angle control parameters.

The first error function tells the driver whether the vehicle is correctly oriented with respect to the ideal path. However, it can be clearly seen that this error function alone is not able to guarantee that the vehicle is following the correct path and not a parallel one. Thus, a second error function was added in order to warn the driver if he is actually driving on the correct path. It should be observed that, while the error function on the vehicle's orientation takes into account the position the vehicle will have l_{steer} meters in front, the error function on the vehicle's position considers the actual position the vehicle. The contribution due to the error function on the vehicle's orientation can therefore be seen as a feed-forward contribution while the one due to the error function on the vehicle's position can be classified as a feed-back contribution. The applied steer wheel angle is a weighted sum of these two contributions:

$$\delta = K_1 \cdot e_1 + K_2 \cdot e_2 \tag{28}$$

where K_1 and K_2 gains are determined as described below.

5.3.1. Feed-forward contribution

For what concerns the feed-forward contribution, the starting point is the kinematic steer angle of the vehicle, i.e. Ackermann's angle defined as

$$\delta_{\text{FF}} \approx \frac{p}{\rho} = \delta_0 \tag{29}$$

where p is the vehicle's wheelbase and ρ is the path radius of curvature (see Fig. 14a). However, as already said, the feed-forward contribution is equal to the error function on the vehicle's orientation

$$\delta_{\text{FF}} = K_1 \cdot e_1 = K_1 \Delta\sigma \tag{30}$$

On a constant radius curve, $\Delta\sigma$ is equal to l_{steer}/ρ. Therefore,

$$\delta_{\text{FF}} \approx K_1 \frac{l_{\text{steer}}}{\rho} \quad \Rightarrow \quad K_1 = K_1(l_{\text{steer}}) = \frac{p}{l_{\text{steer}}} \tag{31}$$

Knowing the vehicle's wheelbase and the "visual distance" the feed-forward contribution of the steer wheel angle can therefore be determined as

$$\delta_{\text{FF}} = K_1(l_{\text{steer}})\Delta\sigma \tag{32}$$

As for the accelerator/brake input, the "visual distance" is a function of both the vehicle speed and the longitudinal acceleration. However, in this case the visual distance depends on actual speed and acceleration values while for the accelerator/brake input the visual distance was a function of reference values:

$$l_{\text{steer}} = V \cdot t_{\text{resp}} + \frac{1}{2} a_x \cdot t_{\text{resp}}^2 \tag{33}$$

Again, the t_{resp} parameter is a function of the driver's behaviour and, in this case, has been determined iteratively in order to optimise the lap time. Fig. 15 shows the influence of such parameter on the vehicle's trajectory. It can be clearly seen that, at increasing t_{resp} value, the driver

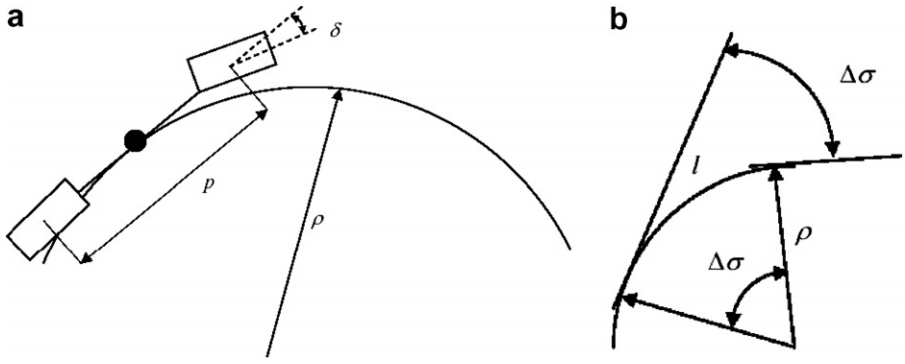

Fig. 14. Kinematic steer angle.

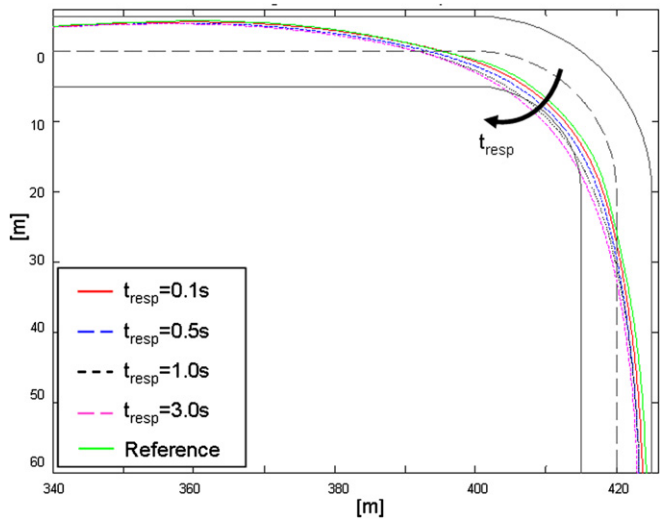

Fig. 15. Influence of t_{resp}.

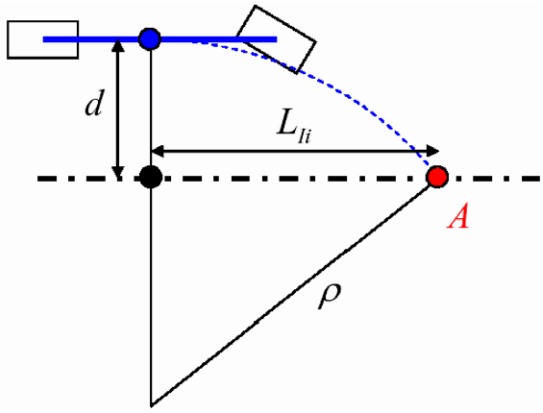

Fig. 16. Control scheme for the correction.

tends to cut away curves thus achieving a higher mean square error for the vehicle's path.

5.3.2. Feed-back contribution

The feed-back contribution allows to correct the asymptotic error of the feed-forward contribution. In fact, as previously described, having zero error on the vehicle's orientation does not mean to have the vehicle on the desired optimal path.

The starting point to determine the feed-back contribution to the steer wheel angle is the same as the feed-forward contribution, i.e. the kinematic steer angle of the vehicle:

$$\delta_{\text{FB}} \approx \frac{p}{\rho} = K_2(d, L_{Ii}) \cdot d \tag{34}$$

Since

$$\rho^2 = L_{Ii}^2 + (\rho - d)^2 \quad \Rightarrow \quad \rho = \frac{L_{Ii}^2 + d^2}{2d} \tag{35}$$

as shown in Fig. 16 $\left(K_2 = \frac{2p}{L_{Ii}^2 + d^2}\right)$.

The parameter L_{Ii} is another "visual distance" that, as before, is proportional to the actual vehicle speed and longitudinal acceleration and has to be determined iteratively:

$$L_{Ii} = V \cdot t_{\text{int}} + \frac{1}{2} a_x t_{\text{int}}^2 \tag{36}$$

Up to now, only the kinematic curving behaviour has been taken into account. However, during fast turns, also the dynamic vehicle's behaviour has to be taken into account.

As shown in Fig. 17, during fast curves also the slip angles at the front (α_1) and at the rear (α_2) axles have to be taken into account. Thus, Eq. (34) becomes:

$$\delta_{\text{dyn}} \approx \frac{p}{\rho} + \alpha_1 - \alpha_2 = \delta_0 + \alpha_1 - \alpha_2 \tag{37}$$

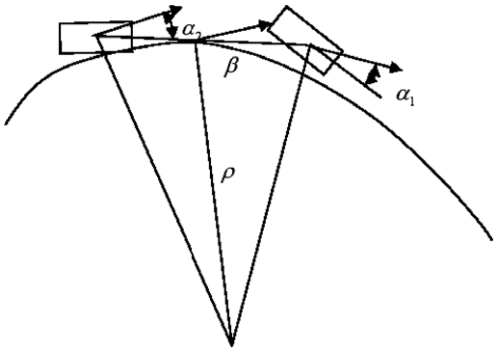

Fig. 17. Tires' slip angle.

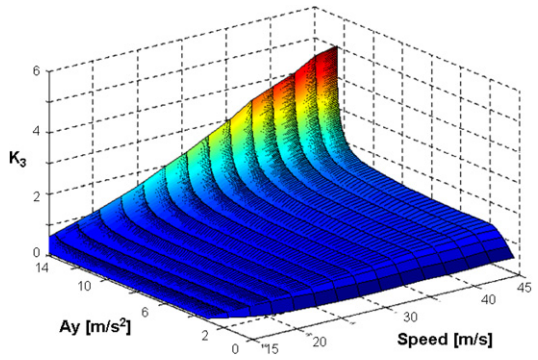

Fig. 18. K_3 vs. lateral acceleration and vehicle speed.

that can be rewritten as

$$\delta_{\mathrm{dyn}} \approx \delta_0 + \alpha_1 - \alpha_2 = \delta_0 + \left(\frac{N_{\mathrm{f}}}{K_{\mathrm{f}}} + \frac{N_{\mathrm{r}}}{K_{\mathrm{r}}}\right) \cdot \frac{V^2}{\rho}$$
$$= \delta_0 + k_{\mathrm{us}} \cdot a_y \quad \Rightarrow \quad \frac{\delta_{\mathrm{dyn}}}{\delta_0} = K_3\left(V, \frac{V^2}{\rho}\right) \tag{38}$$

where N_{f} and N_{r} are the normal loads acting on the front and rear axles respectively, K_{f} and K_{r} are the cornering stiffness of the front and rear tyres respectively and k_{us} is the understeering coefficient. Knowing the kinematic steer angle δ_0 and the vertical loads/cornering stiffness or the understeering coefficient it is possible to determine the K_3

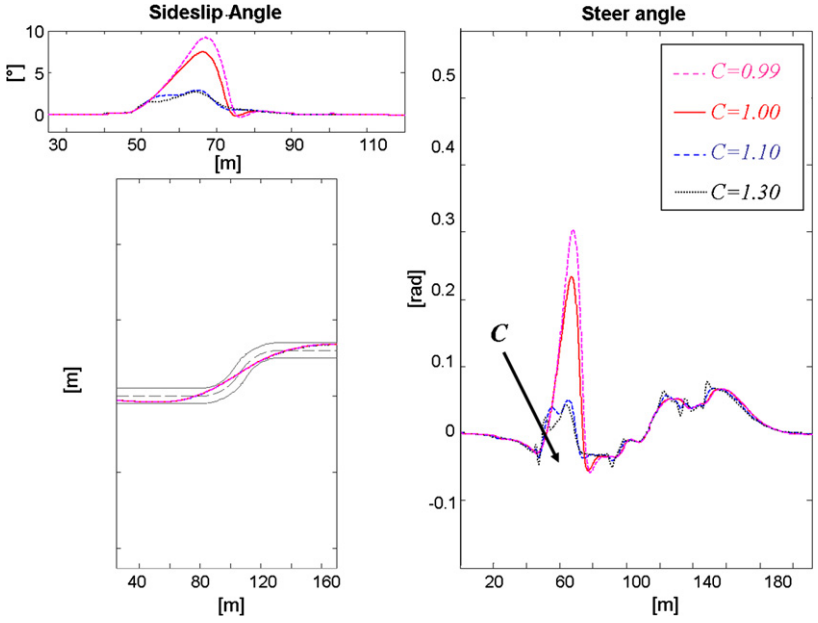

Fig. 19. Influence of K_{tr}.

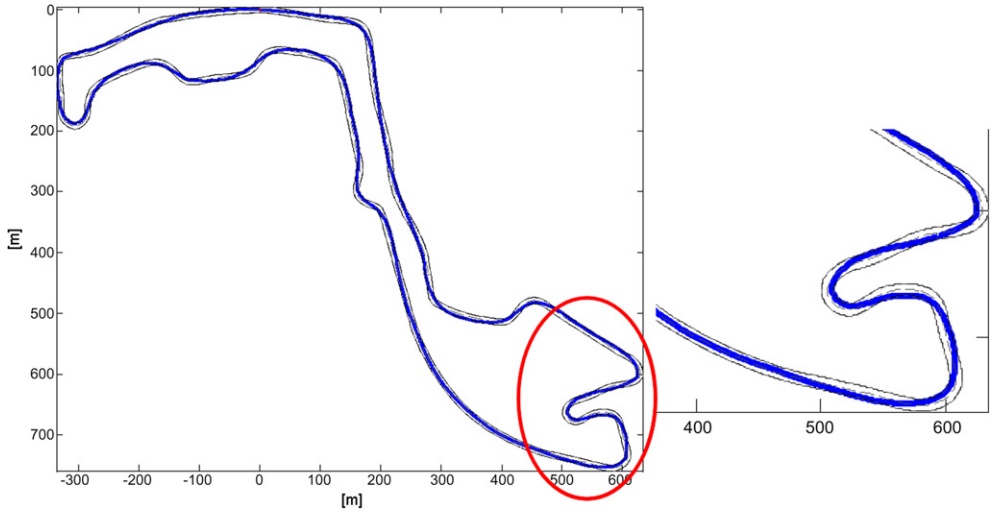

Fig. 20. Montecarlo circuit: ideal path and zoom of the ideal path.

coefficient, a function of the vehicle's speed and of the vehicle's lateral acceleration. As an example, K_3 coefficient is shown in Fig. 18.

Summing up all the terms, the steer wheel angle is equal to

$$\delta = K_3\left(V, \frac{V^2}{\rho}\right) \cdot [K_1(l_{\text{steer}}) \cdot \Delta\sigma + K_2(d, L_{li}) \cdot d] \tag{39}$$

The last effect that has to be considered is the transient behaviour of the vehicle (K_3 coefficient takes into account only the steady state behaviour of the vehicle). This is done by adding a new coefficient K_{tr} a function of the longitudinal vehicle acceleration:

$$\delta = K_{\text{tr}}(a_x) \cdot K_3\left(V, \frac{V^2}{\rho}\right) \cdot [K_1(l) \cdot \Delta\sigma + K_2(d, L_{li}) \cdot d] \tag{40}$$

where

$$K_{\text{tr}}(a_x) = C \cdot |a_x| \tag{41}$$

C being a coefficient that has been determined iteratively. In Fig. 19 the influence of this coefficient is shown: to higher values of C corresponds a smoother behaviour of the driver (see the sideslip angle and the steer angle).

6. Numerical results

Due to the fact that the identification of the driver's inputs has been reduced to a simple quadratic minimization, it is possible to determine the driver's optimal inputs (i.e. the inputs that allow to obtain the best lap time) even on long tracks. Fig. 20 shows the ideal path for the considered vehicle on Montecarlo circuit while Figs. 21 and 22 show the identified driver's inputs. The framed section of Figs. 21 and 22 is referred to the part of the circuit highlighted in Fig. 20.

It can be clearly seen that the driver's inputs are reasonable not nervous. To have a better feeling whether these inputs are correct or not, Fig. 23 shows the vehicle's sideslip angle and the longitudinal/lateral accelerations vs. travelled distance for the considered vehicle on Montecarlo circuit. It can be seen that the sideslip angle never exceeds 3° even in limit conditions.

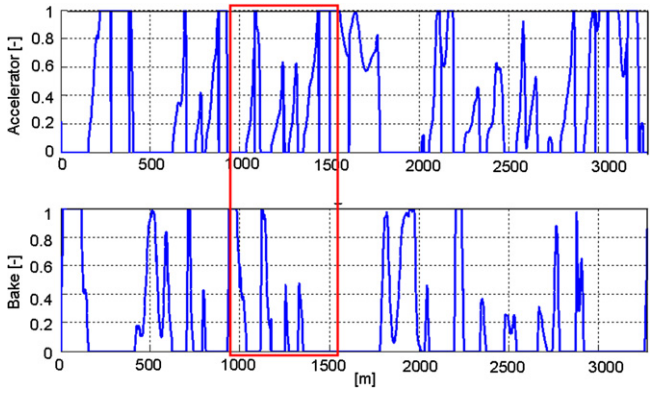

Fig. 21. Montecarlo circuit: accelerator and brake inputs vs. travelled distance.

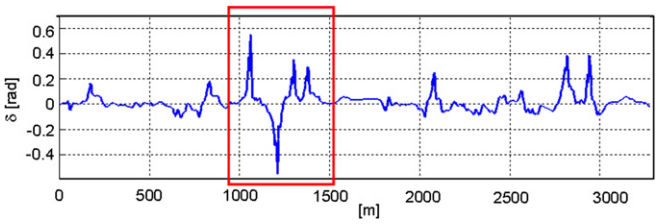

Fig. 22. Montecarlo circuit: steer wheel angle vs. travelled distance.

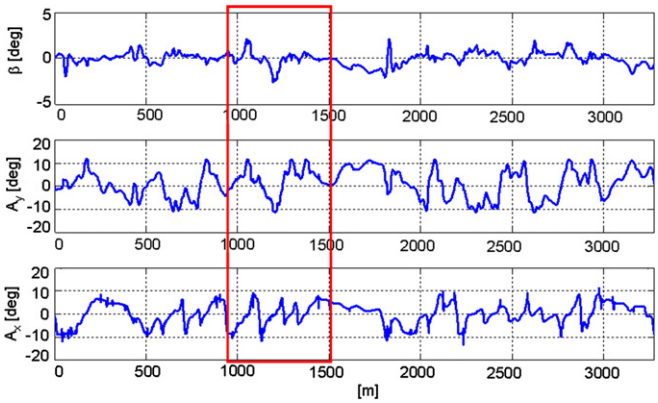

Fig. 23. Montecarlo circuit: lateral and longitudinal acceleration, sideslip angle vs. travelled distance.

7. Conclusions

A fast and reliable algorithm for the identification of the optimal trajectory, both path and speed profile, has been described. This algorithm is based on a series of minimizations that consider both the track geometry and the performances of the considered vehicle.

Once identified the optimal trajectory a identification procedure of the driver's inputs based on a simple quadratic minimization approach has been set up. This procedure allows to carry out the identification even on long tracks such as Montecarlo track. The driver's inputs take into account the vehicle's dynamic behaviour and the driver's characteristics through a series of parameters that, in the present work, were identified to obtain the best lap. However, this parameters can be measured from real drivers thus allowing to compare the driving behaviour and to teach race car driving.

References

[1] Delingette H, Herbert M, Ikeluchi K. Trajectory generation with curvature constraint based on energy minimization. Intelligence for mechanical systems. In: Proceedings IROS, 1991.

[2] Scheuer Laugier. Planning sub-optimal and continuous-curvature paths for car-like robots, In: Proceedings of IEEE/RSJ international conference on intelligent robots and systems, Victoria, Canada, 1998.

[3] Lamiraux F, Lamond JP. Smooth motion planning for car-like vehicles. IEEE Trans Robot Automat 2001;17(4).
[4] Nagy B, Kelly A. Trajectory generation for car-like robots using cubic curvature polynomials. Field and service robots, Helsinki, Finland, 11 June, 2001.
[5] Sharp RS, Casanova D, Symonds P. A mathematical model for driver steering control, with design, turning and performance results. Vehicle Syst Dyn 2000;33:289–326.
[6] Bernard J, Pickelmann M. An inverse linear model of a vehicle. Vehicle Syst Dyn 1986;15(4):179–86.
[7] Cheli F, Leo E, Melzi S, Mancosu F, Giangiulio E, Arosio D. Implementation of a 14 d.o.f. model for the prediction of vehicle dynamics and its interaction with active control systems. Tire Technology Expo 2006, Stuttgart, Germany, 2006.
[8] Cheli F, Leo E, Melzi S, Mancosu F. A 14 d.o.f. model for evaluation of vehicle's dynamics. Int J Mech Control 2005;6(2):19–30.